

Electronic Supplementary Information

Macroscopic Three-dimensional Tetrapod-Separated Graphene-like Oxygenated N-doped Carbon Nanosheets Architecture for Use in Supercapacitors

Can Chen, Guobao Xu, Xiaolin Wei, Liwen Yang*

Hunan Key Laboratory of Micro-Nano Energy Materials and Devices, School of Physics and Optoelectronics, Xiangtan University, Hunan 411105, China

* Corresponding authors: ylwxtu@xtu.edu.cn

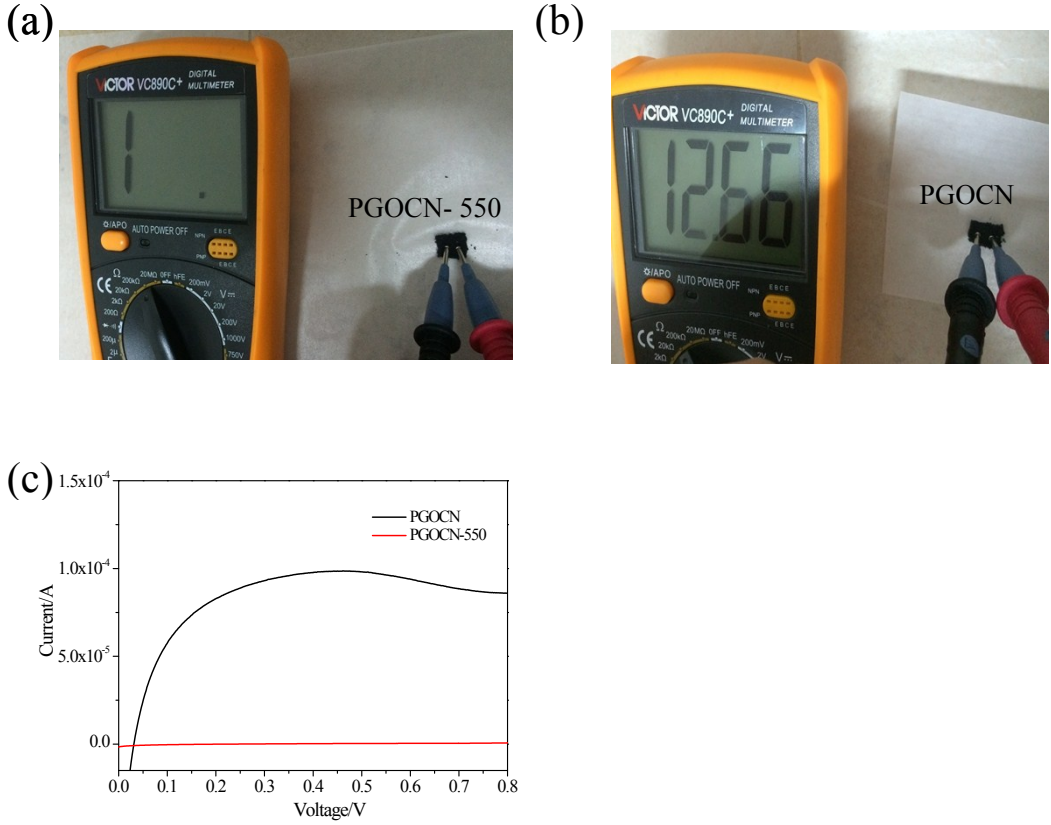
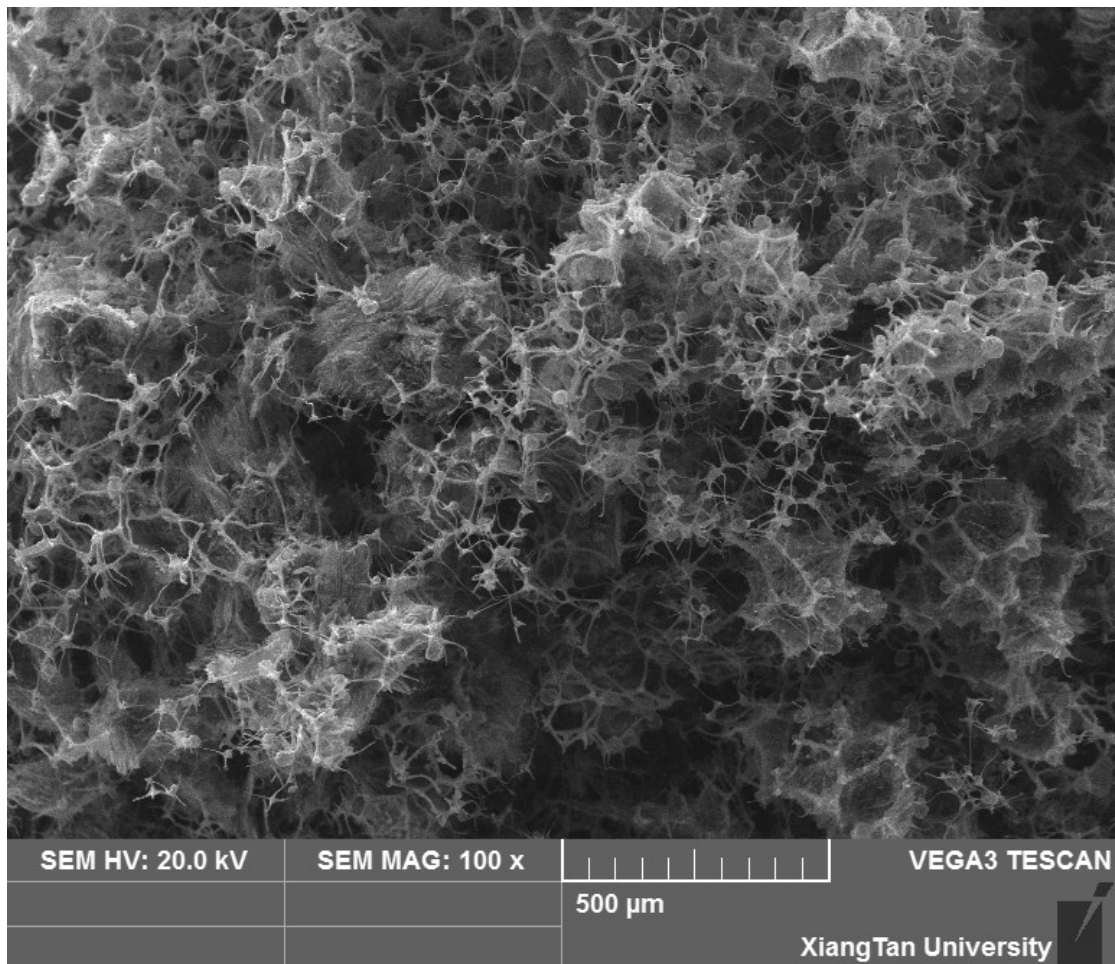


Figure S1. (a)-(b) The measured resistance of the PGOCN-550 and PGOCN material using a multi-meter. The resistance of the PGOCN-550 material is larger than $10^5 \Omega$, while the PGOCN material shows obviously low resistance around $10^4 \Omega$. (c) The CVs in three-electrode system using the PGOCN or referenced PGOCN-550 material as working electrode at the same scanning rate. Higher current can be observed from the PGOCN electrode. The results confirm superior electric conductivity of the PGOCN due to higher carbonization degree compared to the referenced PGOCN-550.



SEM HV: 20.0 kV

SEM MAG: 100 x

500 µm

VEGA3 TESCAN

XiangTan University

Figure S2. Typical SEM image in low magnification of the PGOCN material.

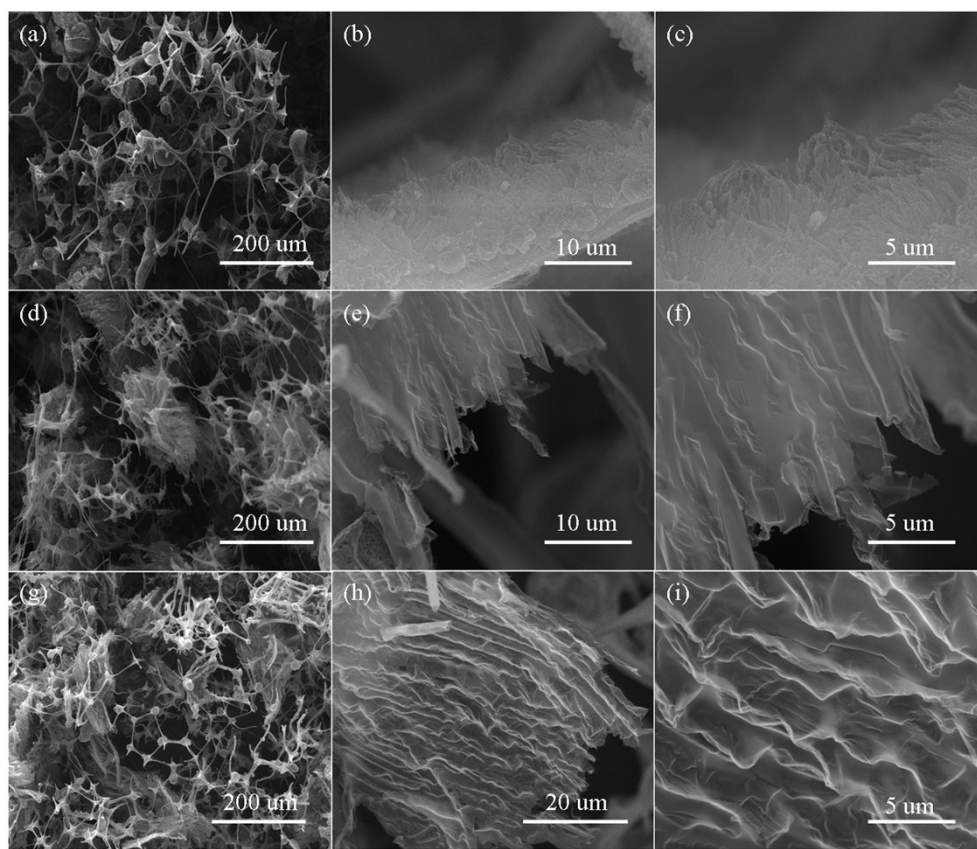


Figure S3. The comparison of typical SEM images acquired from the PCN-550(a)-(c),
PGOCN-550 (d-f) and PGOCN (g-i).

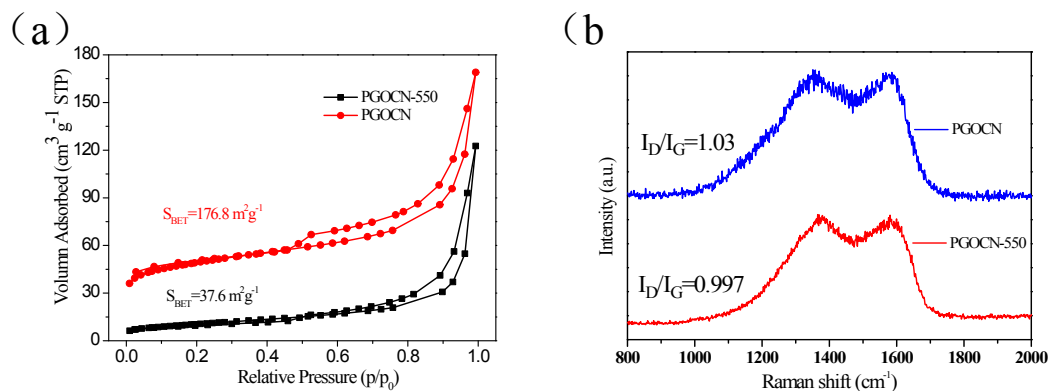


Figure S4. (a) Nitrogen adsorption-desorption isotherm and (b) Raman spectrum of the PGOCN-550 and PGOCN.

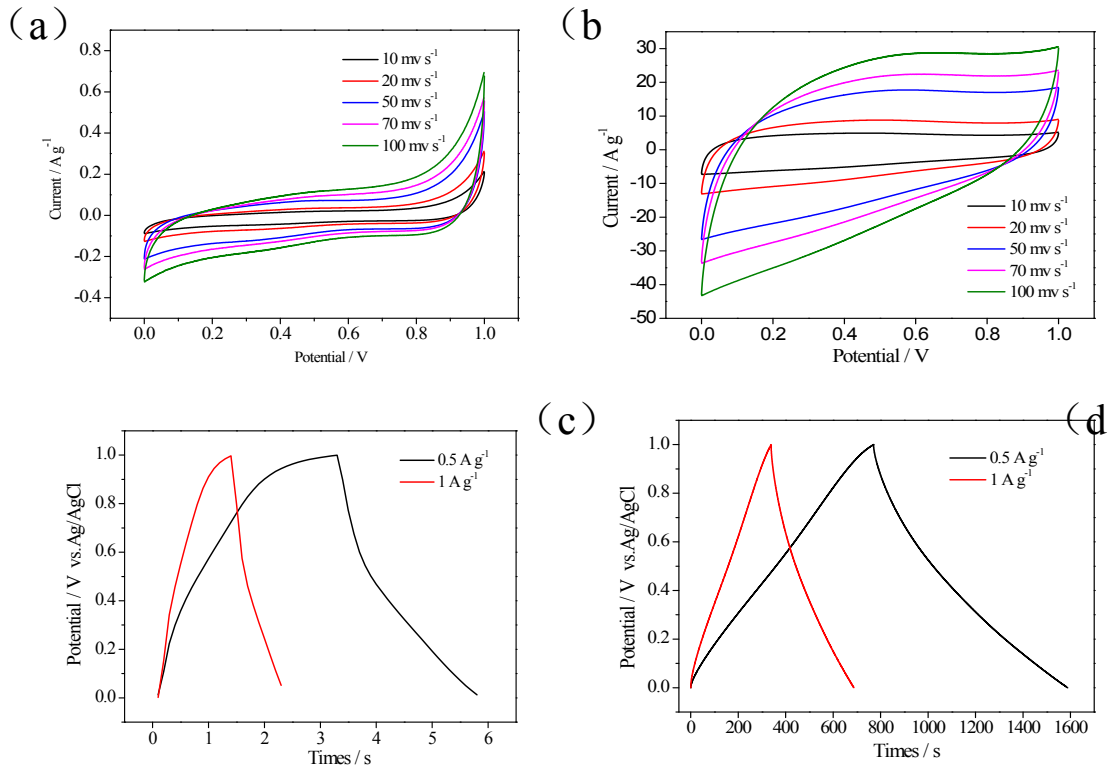


Figure S5. (a)-(b) CVs of the prepared PGOCN-550 and PGOCN in a three-electrode system using 1M H₂SO₄ as electrolyte. (c)-(d) corresponding GCD curves of the prepared PGOCN-550 and PGOCN in a three-electrode system using 1M H₂SO₄ as electrolyte at various current densities.

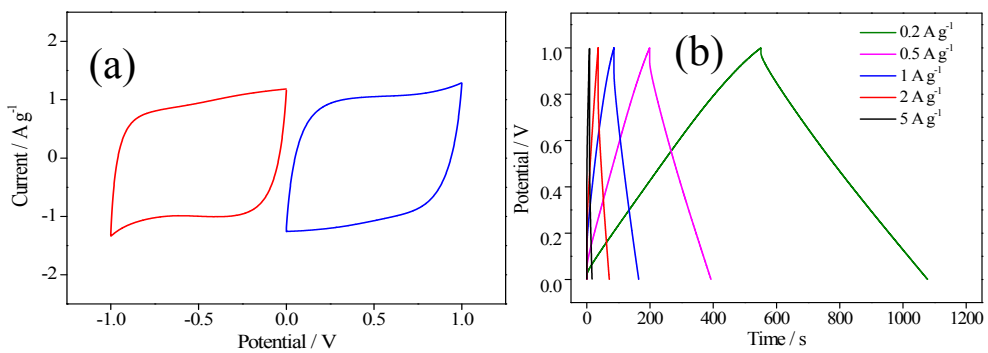


Figure S6. (a) The comparison of CVs for the two-electrode symmetric supercapacitor acquired in the operating voltage of both negative and positive areas at the same scanning rate. (b) GCD curves acquired in the operating voltage of the positive area at various current densities. No obvious difference in specific capacitance was observed.

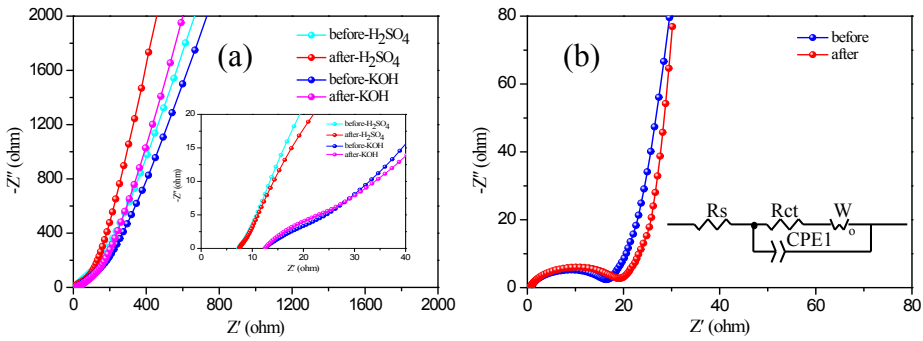


Figure S7. (a) Nyquist plots of PGOCN before/after 2000 cycles in a three-electrode system. The inset of (a) shows enlarged view of high frequency area. (b) Nyquist plots of PGOCN before/after 2000 cycles in a two-electrode PGOCN based symmetric supercapacitor device. The inset of (b) shows the equivalent electrical circuit used to fit the EIS, which includes the electrolyte resistance (R_s), interface charge transfer resistance (R_{ct}), Warburg element (W) and constant phase element (CPE).

Table S1 Comparison of gravimetric capacitances of carbon-based materials as electrodes of supercapacitors, all tested in a three-electrode configuration.

Materials	Capacitance (F/g)	Current density	Electrolyte	ref
RGO@HTC	321	1 A g ⁻¹	6 M KOH	¹
PGF	237	0.2 A g ⁻¹	6 M KOH	²
Activated carbon aerogel	220	0.125 A g ⁻¹	1 M H ₂ SO ₄	³
3D N-B codoped graphene	239	1 A g ⁻¹	1 M H ₂ SO ₄	⁴
N-C-RGO	250	1 A g ⁻¹	6 M KOH	⁵
3D graphene	202	1 A g ⁻¹	1 M Na ₂ SO ₄	⁶
cMR-rGO	203	1 A g ⁻¹	1 M LiPF6	⁷
RGO	190	1 A g ⁻¹	6 M KOH	⁸
PGOCN	348	1 A g ⁻¹	1 M H ₂ SO ₄	This Work
	308	1 A g ⁻¹	6 M KOH	Work

Table S2. Comparison of the rate capability of carbon-based materials as electrodes of two-electrode symmetric cell supercapacitors.

Materials	Current density	Retention ratio (%)	References
RGO@HTC	0.5-10 A g ⁻¹	68	¹
PGF	0.2-10 A g ⁻¹	65	²
HPGM	0.1-15 A g ⁻¹	69	⁹
Polyaniline/graphene film	0.5-10 A g ⁻¹	50	¹⁰
PAF-Carbon	0.2-10 A g ⁻¹	41	¹¹
3D nitrogen-doped porous carbon	0.5-10 A g ⁻¹	58.4	¹²
Interconnected microporous carbon	0.5-30 A g ⁻¹	60	¹³
Meso-microporous activated porous carbon	0.25-10 A g ⁻¹	47.6	¹⁴
Mesoporous graphene	0.5-8 A g ⁻¹	59	¹⁵
PGOCN	0.2-5 A g ⁻¹	80.4	This work

Table S3 Fitting results according to Nyquist plots (see Figure S6b) of the PGOCN based symmetric supercapacitor device

Sample(PGOCN)	$R_s(\Omega)$	$R_{ct}(\Omega)$	W	CPE
Before Cycling	0.58	16.09	0.44372	0.7671
After Cycling	0.66	18.58	0.44925	0.7679

References:

1. H. Luo, Z. Liu, L. Chao, X. Wu, X. Lei, Z. Chang and X. Sun, *J. Mater. Chem.A*, 2015, 3, 3667-3675.
2. K. Yuan, Y. Xu, J. Uihlein, G. Brunklaus, L. Shi, R. Heiderhoff, M. Que, M. Forster, T. Chassé and T. Pichler, *Adv. Mater.*, 2015, 27, 6714-6721.
3. Z. Zapata-Benabithe, F. Carrasco-Marín and C. Moreno-Castilla, *J. Power Sources*, 2012, 219, 80-88.
4. Z. S. Wu, A. Winter, L. Chen, Y. Sun, A. Turchanin, X. Feng and K. Müllen, *Adv. Mater.*, 2012, 24, 5130-5135.
5. Y. Ren, J. Zhang, Q. Xu, Z. Chen, D. Yang, B. Wang and Z. Jiang, *RSC Adv.*, 2014, 4, 23412-23419.
6. B. G. Choi, M. Yang, W. H. Hong, J. W. Choi and Y. S. Huh, *ACS nano*, 2012, 6, 4020-4028.
7. J. H. Lee, N. Park, B. G. Kim, D. S. Jung, K. Im, J. Hur and J. W. Choi, *ACS nano*, 2013, 7, 9366-9374.
8. Z. Lei, L. Lu and X. Zhao, *Energy Environ. Sci.*, 2012, 5, 6391-6399.
9. Y. Tao, X. Xie, W. Lv, D.-M. Tang, D. Kong, Z. Huang, H. Nishihara, T. Ishii, B. Li and D. Golberg, *Sci. Rep.*, 2013, 3, 2975.
10. Z. Tong, Y. Yang, J. Wang, J. Zhao, B.-L. Su and Y. Li, *J. Mater. Chem.A*, 2014, 2, 4642-4651.
11. Z. Xiang, D. Wang, Y. Xue, L. Dai, J.-F. Chen and D. Cao, *Sci. Rep.*, 2015, 5, 8307.
12. J. Pu, C. Li, L. Tang, T. Li, L. Ling, K. Zhang, Y. Xu, Q. Li and Y. Yao, *Carbon*, 2015, 94, 650-660.
13. D. Puthusseri, V. Aravindan, S. Madhavi and S. Ogale, *Energy Environ. Sci.*, 2014, 7, 728-735.
14. S. Song, F. Ma, G. Wu, D. Ma, W. Geng and J. Wan, *J. Mater. Chem.A*, 2015, 3, 18154-18162.
15. C. Liu, Z. Yu, D. Neff, A. Zhamu and B. Z. Jang, *Nano Lett.*, 2010, 10, 4863-4868.